FLORE
Repository istituzionale dell'Università degli Studi di Firenze

Solitary Necrotic Nodules of the Liver: Cross-Sectional Imaging Findings and Follow-Up in Nine Patients

(Article begins on next page)

19 April 2024

Solitary Necrotic Nodules of the Liver: Cross-Sectional Imaging Findings and Follow-Up in Nine Patients

Stefano Colagrande[1]
Maria Lara Paolucci[1]
Luca Messerini[2]
Wolfgang Schima[3]
Alfred Stadler[3]
Tommaso Vincenzo Bartolotta[4]
Angelo Vanzulli[5]
Giuseppe Brancatelli[4,6]

[1]Department of Clinical Physiopathology, Section of Radiodiagnostics, University of Florence, Viale Morgagni 85, Azienda Ospedaliero-Universitaria Careggi, 50134 Florence, Italy. Address correspondence to S. Colagrande (stefano.colagrande@unifi.it).

[2]Department of Human Pathology and Oncology, University of Florence, Florence, Italy.

[3]Department of Radiology, Medical University of Vienna, Vienna, Austria.

[4]Department of Radiology, University of Palermo, Palermo, Italy.

[5]Department of Diagnostic and Interventional Radiology, Niguarda Ca Granda Hospital, Milan, Italy.

[6]Department of Radiology, University of Pittsburgh School of Medicine, Pittsburgh, PA.

OBJECTIVE. The purpose of our study was to retrospectively evaluate the sonographic, CT, and MRI findings (number, diameter, lobar location, depth from the hepatic capsule, and appearance of lesions) in a series of nine patients with pathologically proven solitary necrotic nodules of the liver and the natural evolution at follow-up in four of the nine patients.

CONCLUSION. Solitary necrotic nodules are usually small, solitary lesions, mainly located under the liver capsule of the right lobe. They are hypoechoic on sonography, hypoattenuating on CT, have low signal intensity on both T1- and T2-weighted MRI with lack of enhancement after IV contrast administration, and at follow-up have a tendency to show calcification and involution toward reduction in size.

S olitary necrotic nodule of the liver is a rare benign lesion reported in the pathology and radiology literature [1–21] and might result from previous trauma, parasite infection, or hemangioma [1–6]. At pathology, it is characterized by a necrotic central core surrounded by a dense hyalinized fibrotic capsule. Previous authors have shown that solitary necrotic nodule of the liver has sometimes been misinterpreted as malignant [5–8], leading to inappropriate treatment. To that end, awareness and recognition of this entity have important implications for patient care to avoid errors in management. The existing knowledge of the imaging features of solitary necrotic nodule of the liver is gleaned mostly from articles describing one or two patients [1–20], and the only case series investigates the imaging features of solitary necrotic nodules of the liver with histopathology [4, 7] or sonography only [21]. To our knowledge, no case series describing the imaging features of solitary necrotic nodules with cross-sectional imaging has been reported except an article that was recently published in the non-English-language literature [22]. Moreover, because the numbers of patients with solitary necrotic nodule of the liver are small, no information exists on the natural history. With the nine patients with solitary necrotic nodule of the liver reviewed here, we will expand on the information gained from prior studies.

The purpose of this retrospective study was therefore to evaluate the imaging features at cross-sectional imaging in a series of patients with solitary necrotic nodule of the liver, and to describe the natural evolution at follow-up for 2–6 years after histologic diagnosis. Two of these patients were included in an earlier report that focused on the imaging features [16] but not on the natural history of the nodules.

Materials and Methods
Patients
The imaging examinations of nine patients with pathologically proven solitary necrotic nodule of the liver were included in this study. Proof of diagnosis was based on findings at core-biopsy performed with an 18-gauge needle ($n = 6$) or at liver resection ($n = 3$). Cases were collected from four university hospitals over a 6-year period and were identified by reviewing pathology databases.

In our patients, solitary necrotic nodules were incidentally detected on cross-sectional imaging performed for various reasons, such as staging in patients with extrahepatic primary malignancies ($n = 3$), abdominal pain ($n = 3$), and suspected gallbladder ($n = 2$) or urinary ($n = 1$) stones. Institutional review board approval and patient consent were not required for this retrospective study because patient privacy was maintained and patient care was not impacted.

Imaging Protocols and Methods
Sonography was performed in six patients with two scanners (Astro MP, Esa Ote-Ansaldo or HDI

TABLE 1: Synopsis of Demographics and Imaging Findings in Nine Patients with Solitary Necrotic Nodules of Liver

| | Patient | | Nodule Size (mm) | Proof of Diagnosis | Segment (Site) | Calcification | Sonographic Echogenicity[a] | CT Attenuation | | MRI Signal Intensity | | | Changes at Follow-Up |
No.	Age (y)	Sex						Unenhanced[b]	CE	T1[c]	T2[c]	CE	
1	75	M	10	Resection	VII (subcapsular)	Yes	Hyper	Hyper	No	—	—	No	—
2	51	F	10	Resection	VII (≈ 1 cm from capsule)	Yes	Hyper	—	No	—	—	No	—
3	61	M	10	Resection	VI (subcapsular)	No	Hypo	Hypo	No	—	—	No	—
4	30	F	15(I), 10 (FU)	Biopsy	VI (subcapsular)	No (I), yes (FU)	Hypo (I), hyper (FU)	Hypo (I), hyper (FU)	No	Hypo	Hypo	No	Calcification and size reduction
5	40	M	30 (I), 22 (FU)	Biopsy	VI (subcapsular)	No (I), yes (FU)	Hypo (I), hyper (FU)	Iso (I), hyper (FU)	No	Hypo	Hypo	No	Calcification and size reduction
6	37	F	22 (I), 12 (FU)	Biopsy	VII–VIII (≈ 1 cm from capsule)	No (I), yes (FU)	Hypo (I), hyper (FU)	Hypo (I), hyper (FU)	No	Iso	Hypo	No	Calcification and size reduction
7	38	F	38	Biopsy	VII (subcapsular)	No	—	Hypo	No	Hypo	Iso	No	—
8	69	F	10 (I), 7 (FU)	Biopsy	VIII (> 1 cm from capsule)	No (I), no (FU)	—	Hypo	No	Hypo	Iso	No	Size reduction
9	66	F	40, 18, 10	Biopsy	VI (subcapsular)	No	—	Hypo	No	—	—	No	—

Note—Dash (—) indicates not applicable, CE = contrast-enhanced, I = initial, FU = follow-up.
[a]Hyper = hyperechoic, hypo = hypoechoic.
[b]Hyperattenuating, hypo = hypoattenuating, iso = isoattenuating.
[c]Hypo = hypointense, iso = isointense.

5000, ATL), with 2- to 5-MHz multifrequency curvilinear transducers and frequencies selected to optimize imaging of the liver. Color or power Doppler sonography was not performed.

Helical multiphasic CT was performed in eight patients using Somatom Plus Volume Zoom 4 (Siemens Medical Solutions) and Brilliance-40 (Philips Healthcare) units with 3- to 7-mm contiguous sections. After unenhanced acquisitions of the liver, patients underwent helical multiphase CT that included both hepatic arterial phase and portal venous phase imaging (25–30 seconds and 70 seconds, respectively), after IV infusion of 1.5 mL/kg of body weight of nonionic contrast material (iopromide, Ultravist 370, Bayer Schering Pharma or iohexol, Omnipaque 300, GE Healthcare). Contrast material was injected at a rate of 3–5 mL/s with a mechanical power injector (Envision CT, MEDRAD).

MRI was performed in five patients with various 1.5-T MR units (Gyroscan ACS NT, Infinion, or Intera; Philips Healthcare or Magnetom Vision, Siemens Medical Solutions) with a body or phased-array receive coil. A breath-hold T1-weighted gradient-recalled echo pulse sequence (called FFE on the Philips systems and called FLASH on the Siemens systems) was performed. The acquisition parameters on the scanners from Siemens Medical Solutions were TR/TE, 177/4; flip angle, 80°; field of view, 38 cm; matrix, 256 × 256; number of sections, 20;

section thickness, 8 mm; and one signal acquired. The acquisition parameters on the scanners from Philips were TR range/TE range, 146–216/1.5–2.0; flip angle, 80°; field of view, 36–40 cm; matrix, 256 × 192; number of sections, 24; section thickness, 6 mm; and one signal acquired. A respiratory-triggered T2-weighted fast spin-echo fat-saturated pulse sequence was also performed. Siemens acquisition parameters were as follows: 4000/ 88; echo-train length, 33; flip angle, 80°; field of view, 38 cm; matrix, 256 × 256; number of sections, 20; section thickness, 8 mm; and one signal acquired. Philips acquisition parameters were as follows: 810–970/80–210; echo-train length, 61; field of view, 36–40 cm; matrix, 256 × 192; number of sections, 48; section thickness, 4 mm; and one signal acquired.

The following contrast agents were used. Ferumoxides particles (Endorem, Guerbet) were injected in one patient. Non-liver-specific gadolinium chelates ([gadopentetate dimeglumine] Magnevist, Bayer Schering Pharma and [gadodiamide] Omniscan, GE Healthcare) were injected in five patients, one of whom also had administration of mangafodipir trisodium (Teslascan, GE Healthcare) during the same examination and gadoxate (Primovist, Bayer Schering Pharma) at follow-up. After manual IV bolus administration of 0.2 mL/kg of body weight of nonspecific gadolinium chelates, T1-weighted dynamic gradient-recalled echo sequences were performed

again during the hepatic arterial and portal venous phases, at 20 seconds and 60 seconds. A delayed acquisition at 4 minutes (range, 3–5 minutes) was added. T1-weighted gradient-recalled echo images were obtained 20 minutes after the start of mangafodipir trisodium infusion or gadoxate bolus administration. After IV infusion over 30 minutes of 6 mL of ferumoxides diluted in 100 mL of saline solution, a T2-weighted fat-saturated turbo spin-echo sequence was performed.

Image Analysis

Imaging studies were evaluated on film by two abdominal radiologists (with experience ranging from 4 to 20 years) in consensus in each contributing institution and then reevaluated by a study coordinator (with 20 years of experience). Readers were not blinded to the pathology results. When the reviewers and the coordinator expressed discordant opinions, they reached a consensus through a joint review of the recorded images. Six patients underwent sonography; eight patients, CT; and five patients, MRI. Four patients underwent serial examinations.

The following imaging criteria were analyzed: number of lesions; lesion diameter; lesion location according to the hepatic segment numbering system of Couinaud [23]; measurements of the depth of the lesion, obtained by measuring the greatest distance from the hepatic capsule (a lesion was arbitrarily classified as deep or subcapsular

when located > 10 or ≤ 10 mm from the hepatic surface, respectively); sonographic pattern, classified as hypoechoic, isoechoic, or hyperechoic to the adjacent liver parenchyma; attenuation at unenhanced and contrast-enhanced CT, classified as hypoattenuating, isoattenuating, or hyperattenuating to the adjacent liver parenchyma; signal intensity characteristics of the lesions at unenhanced and contrast-enhanced T1-weighted MRI with regard to the surrounding liver par-

enchyma; and presence and pattern of calcifications, defined as discrete, strongly hyperattenuating foci on unenhanced CT images. In those four patients who underwent serial examinations, we evaluated the evolution of the imaging appearance of the nodules. The nontumorous liver was evaluated for the presence of liver steatosis or cirrhosis. The grade of liver steatosis was defined as absent, mild (0–10%), moderate (>10–30%), or severe (>30%).

Pathology

All cases were reviewed retrospectively by one pathologist with expertise in hepatic pathology. Microscopic examination was performed on paraffin-embedded representative sections of the lesions, which were routinely processed and stained with H and E, and cytologic aspects of hepatocytes were noted. Special stains, such as elastic van Gieson, reticulin, Grocott-Gomori, Ziehl-Neelsen, and periodic acid–Schiff were also
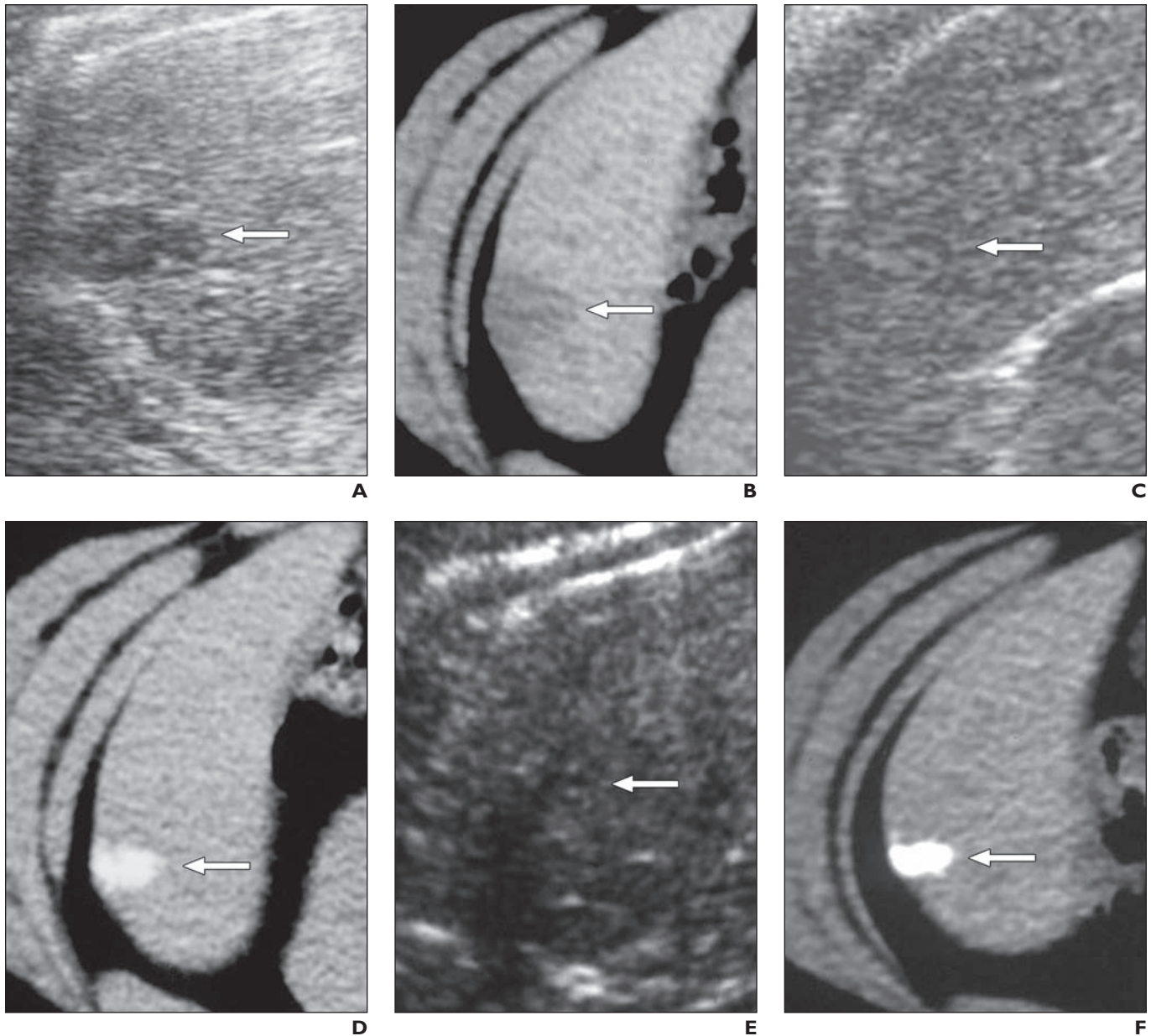
Fig. 1—30-year-old woman with subcapsular solitary necrotic nodule in right lobe of liver (patient 4).
A and **B,** Nodule (*arrow*) in segment VI is hypoechoic on sonogram (**A**) and hypoattenuating on unenhanced CT scan (**B**).
C and **D,** At 2-year follow-up, nodule (*arrow*) is isoechoic and difficult to distinguish from surrounding parenchyma on sonogram (**C**). Unenhanced CT scan (**D**) shows involution into calcification (*arrow*).
E and **F,** At 5-year follow-up, nodule appears slightly hyperechoic and not well identifiable on sonogram (**E**); acoustic shadowing from calcification is seen (*arrow*). On CT scan (**F**), nodule (*arrow*) appears more calcified and smaller in comparison with **D**.

performed in selected cases. The morphologic diagnosis was based on the presence of a central homogeneous eosinophilic necrotic area surrounded by a thin boundary of connective tissue [6, 7, 15, 16].

Results

The main findings are summarized in Table 1. There was no history of trauma, parasite infection, or hemangioma in any of the patients. Eight patients had a single nodule, whereas one patient had a cluster of three nodules. Lesions had a mean diameter of 16 mm (range, 10–40 mm). Lesions were found in the right lobe in all cases. Nodules were located at a distance of ≤ 10 mm from the liver capsule in all but one case.

Sonography

At sonography, noncalcified lesions were hypoechoic, whereas calcified lesions were hyperechoic (Fig. 1) in comparison with the surrounding liver.

CT

At unenhanced CT, lesions were hypoattenuating to the surrounding liver, except for calcified lesions that were hyperattenuating to the surrounding liver (Figs. 1–3) and for a single lesion that was nearly isoattenuating because there was steatosis of the surrounding liver (Fig. 2). No enhancement was observed after IV contrast injection in any case.

MRI

At MRI, nodules were hypointense on both T1- and T2-weighted images except for a single case that was nearly isointense on T1-weighted images (Fig. 3). None of the nodules showed enhancement after gadolinium injection (Fig. 3). In the patient who had images acquired after ferumoxides injection, loss of signal intensity was observed in the liver parenchyma but not in the solitary necrotic nodule. No signal change of the solitary necrotic nodule was observed in the patient who had images acquired after manganese injection. In one patient who underwent mangafodipir- and gadoxate-enhanced MRI, no enhancement of the lesion in the liver-specific phase was observed.

Follow-Up and Calcified Nodules

Imaging follow-up was available in four cases and ranged from 2 to 6 years. Nodules became smaller (*n* = 4) and calcified (*n* = 3) (Table 1). Two solitary necrotic nodules

without follow-up imaging were also calcified. Therefore, a total of five solitary necrotic nodules were calcified. Calcifications involved the entire lesion in all cases and appeared either as homogeneously dense masses (Fig. 1) or with an outer rim of increased attenuation and a central core of less-intense hyperattenuation (Figs. 2 and 3).

Pathology

With regard to the presence and degree of liver steatosis, eight patients had normal findings, whereas one patient was considered to have moderate steatosis.

Despite intense retrospective review, no cause could be established for any of the lesions. All solitary necrotic nodules were composed of a central eosinophilic necrotic area surrounded by a collagenous rim with a variable number of elastic fibers and a scant number of mononuclear inflammatory cells. The necrotic core showed the histologic features of the coagulative necrosis: dehydration and intense cytoplasmic eosinophilia of the dead cells (Fig. 4), and it varied as a consequence of the presence or absence of calcifications, nuclear debris, and ghost or inflammatory cells.

A massive calcification of the necrotic area was found in two patients (Fig. 4). Scarce nuclear debris and rare mononuclear inflammatory cells were present in the central area in another patient. The necrotic core showed some nuclear debris and a large number of mononuclear inflammatory cells in another patient. In no cases were vessels

A

B
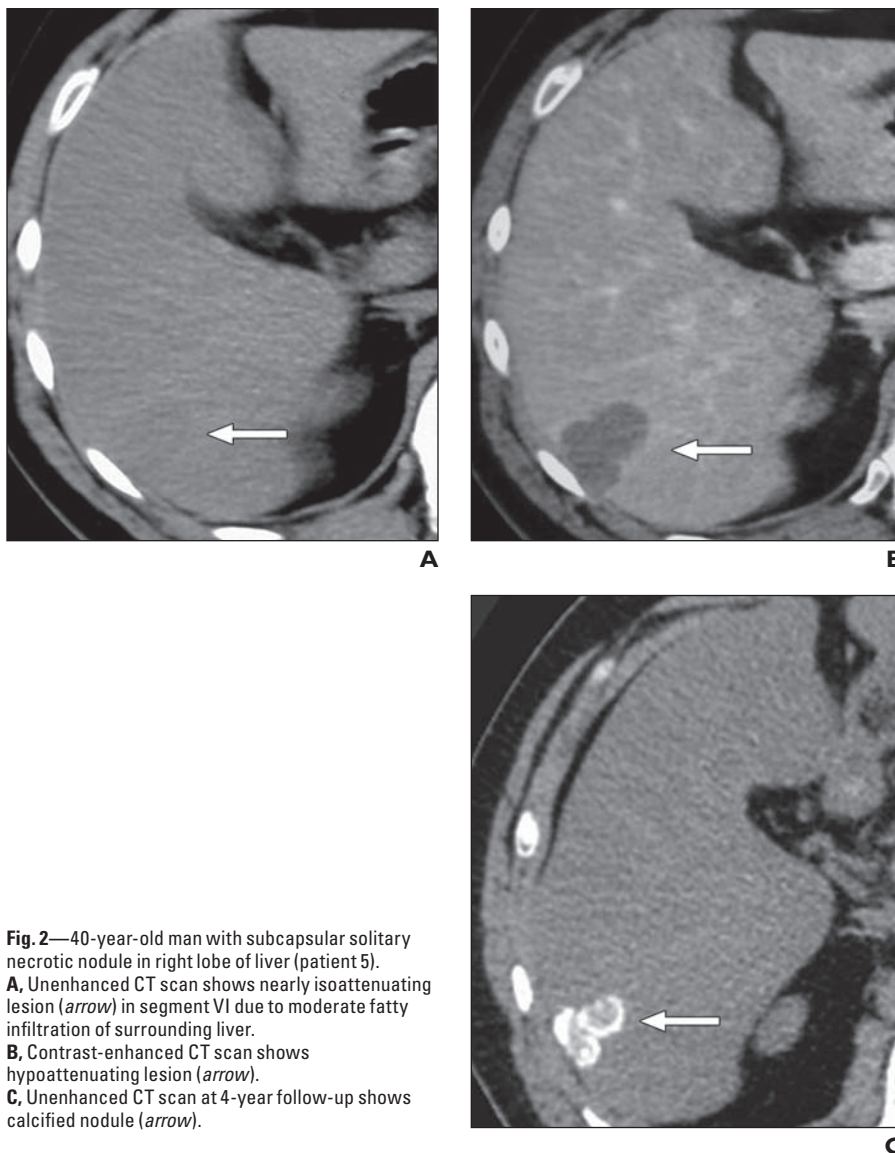
Fig. 2—40-year-old man with subcapsular solitary necrotic nodule in right lobe of liver (patient 5).
A, Unenhanced CT scan shows nearly isoattenuating lesion (*arrow*) in segment VI due to moderate fatty infiltration of surrounding liver.
B, Contrast-enhanced CT scan shows hypoattenuating lesion (*arrow*).
C, Unenhanced CT scan at 4-year follow-up shows calcified nodule (*arrow*).

C
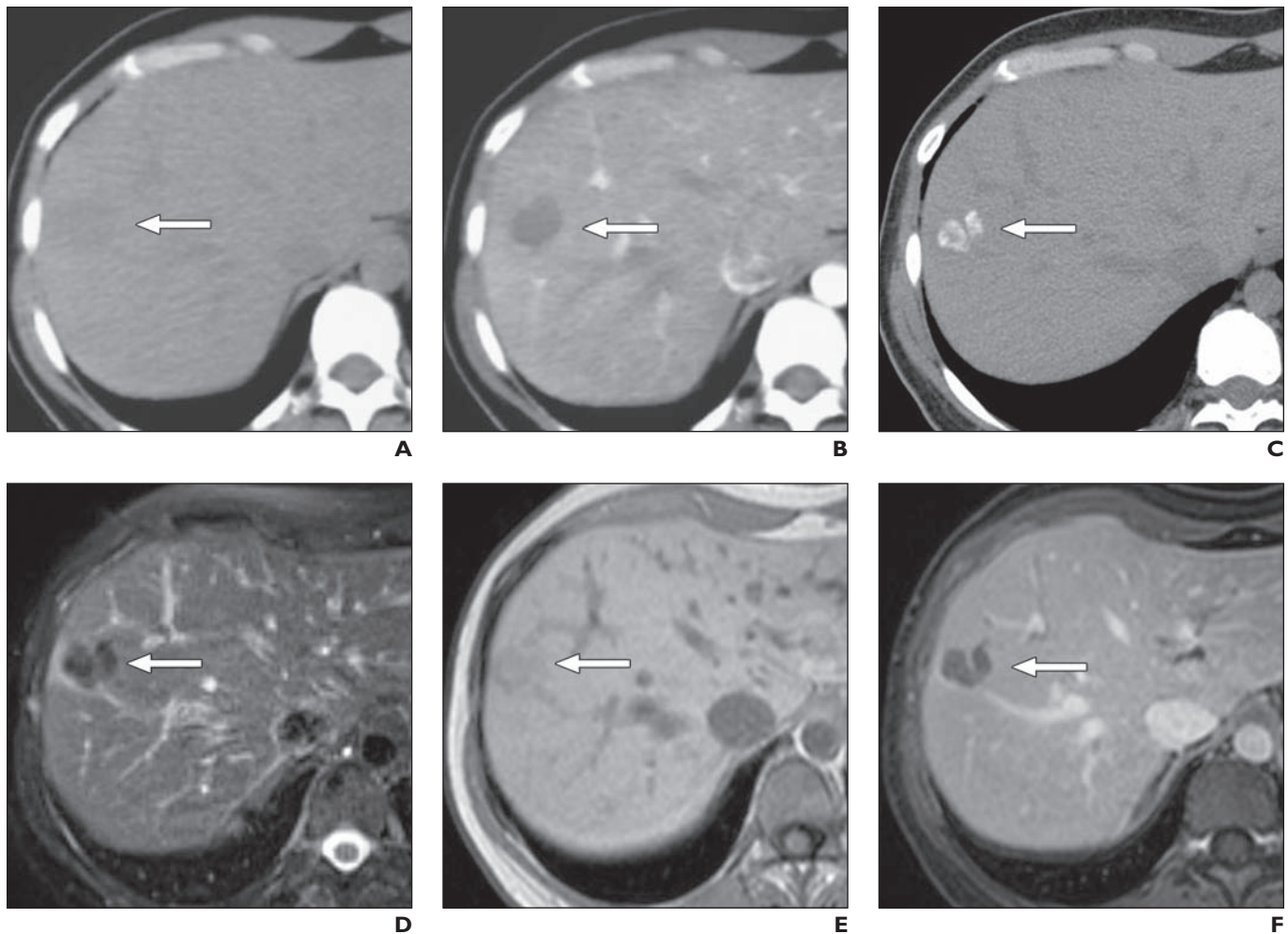
Fig. 3—37-year-old woman with solitary necrotic nodule in right lobe of liver (patient 6).
A–C, Unenhanced (**A**) and contrast-enhanced (**B**) CT scans show subcapsular hypoattenuating lesion (*arrow*). Nodule is calcified (*arrow*) on 2-year follow-up CT scan (**C**).
D–F, MRI performed at same time as **C** shows lesion (*arrow*) as hypointense and nearly isointense to surrounding liver parenchyma on transverse T2-weighted fat-suppressed turbo spin-echo (**D**) and T1-weighted gradient-echo (**E**) images, respectively. T1-weighted gadolinium-enhanced gradient-echo MR image (**F**) shows no contrast enhancement within lesion (*arrow*).

shown, and the hepatic tissue surrounding the lesions was normal. Special stains, such as Grocott-Gomori, Ziehl-Neelsen, and periodic acid-Schiff, excluded bacterial, fungal, and parasitic infections.

Discussion

The imaging and histologic findings in the nine patients reported herein reaffirm those of previous studies and put some others into question. In our series, solitary necrotic nodules were located in a subcapsular area of the right lobe of the liver in all but one case. These characteristics are in accordance with the existing literature. Among 60 cases reported in the literature, 73% were right-sided and 62% were subcapsular [1–6, 8–10, 12–21]. In this study, we found a single lesion in eight of nine patients and a cluster of

three lesions in one patient. Occurrence of more than one nodule in the same patient has been reported in only three studies [3, 10, 14]. In our series, the mean diameter of solitary necrotic nodules was 16 mm, which is in accordance with the mean diameter of 17.6 mm reported by previous authors [1–6, 8–10, 12–21].

Imaging findings of solitary necrotic nodules in the literature are scant and have mostly involved single cases. Solitary necrotic nodules imaged in our study were typically hypointense on both T1-weighted and T2-weighted imaging, which is not surprising in consideration of the dehydrated, coagulative necrosis observed at histopathology. We were interested in the observation that our pathologists defined the necrosis of solitary necrotic nodules as "coagulative" [24, 25], a

finding that has been typically described in the literature as a consequence of previous treatment with ablative techniques [26] and only occasionally observed in untreated lesions [27, 28].

Lack of enhancement after IV contrast injection reflects the avascular nature of solitary necrotic nodules found at histology in this study. We believe that the imaging findings reported in this study proved to be nonspecific for characterization of solitary necrotic nodules. Numerous reports on solitary necrotic nodules misdiagnosed those as hypovascular metastatic lesions [5–8]. Even the use of ferumoxides, mangafodipir, and gadoxate in two of our cases did not allow a specific diagnosis because solitary necrotic nodules share the lack of uptake of liver-specific agents with liver metastases.
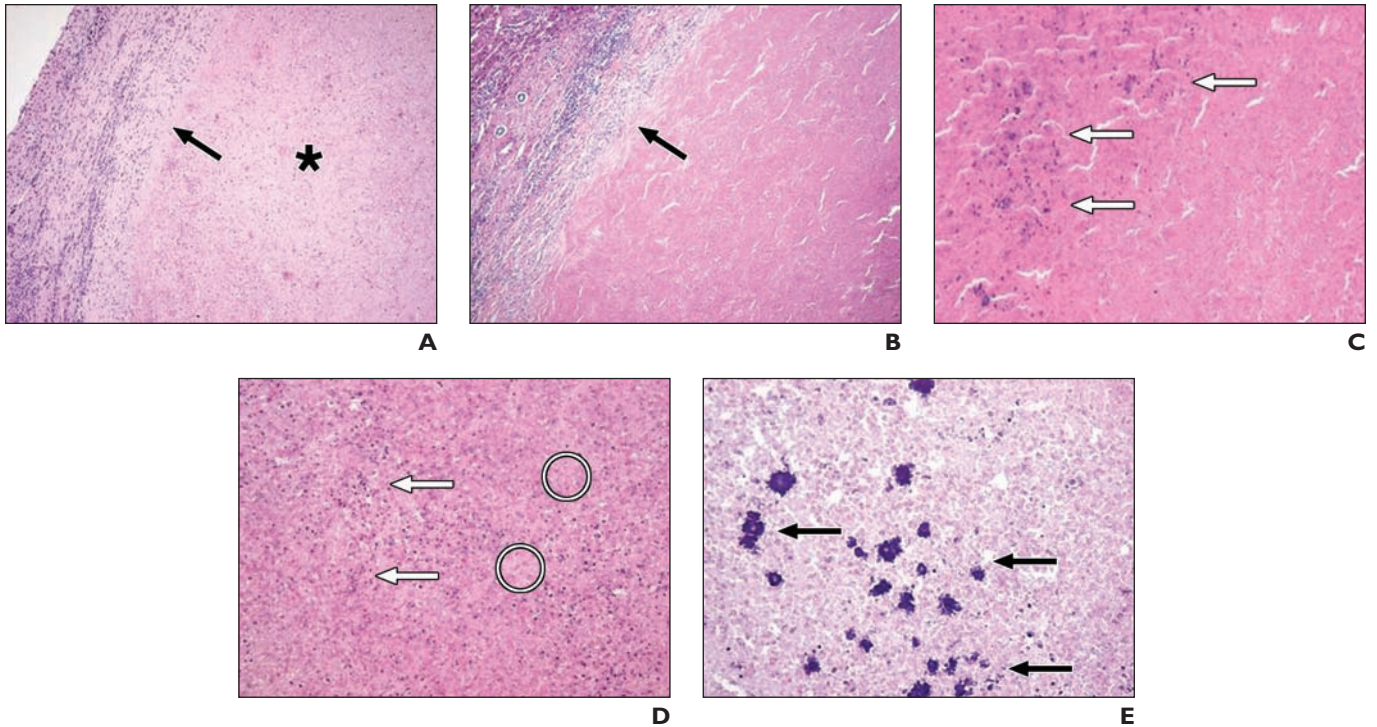
Fig. 4—Histopathologic features of various noncalcified and calcified solitary necrotic nodules of liver.

A and **B**, Photomicrographs from 30-year-old woman with subcapsular solitary necrotic nodule in right lobe of liver (patient 4). Lesion consists of core of eosinophilic coagulative necrosis (*asterisk*) clearly separated from surrounding liver tissue by rim of collagenous tissue (*arrows*). (H and E, ×100)

C, Photomicrograph from 40-year-old man with subcapsular solitary necrotic nodule in right lobe of liver (patient 5) shows necrotic area containing some inflammatory mononuclear cells (*arrows*). (H and E, ×200)

D, Photomicrograph from 37-year-old woman with solitary necrotic nodule in right lobe of liver (patient 6) shows large number of mononuclear inflammatory cells (*arrows*) and some nuclear debris (*circles*) in necrotic area. (H and E, ×200)

E, Photomicrograph from 75-year-old man with subcapsular solitary necrotic nodule (patient 1). Central necrotic core due to coagulative necrosis shows several calcium depositions (*arrows*). Different tone of this photomicrograph in comparison with **A–C** is due to different time of tissue fixation. (H and E, ×200)

In our experience, the key findings that might increase the ability of radiologists to suspect a diagnosis of solitary necrotic nodules are the complete lack of enhancement, both in the center and in the periphery, after contrast agent administration (although most metastases do not show hypervascularity, they are all fed by the hepatic artery and will indeed show some peripheral rim enhancement after contrast injection) [29] and hypointensity on T2-weighted images (metastases will show hyperintensity on T2-weighted images in most cases) [30].

The differential diagnosis between solitary necrotic nodules and liver metastases has important implications for patient care. Whereas the first warrants conservative management, the second are usually treated with resection or chemotherapy.

According to previously published reports, solitary necrotic nodules are not a specific pathologic entity but a consequence of different conditions such as trauma, hemangioma, or parasite infestation [4, 7]. Despite intense retrospective review of histopathology specimens, the cause remained unknown in our patients. We speculate that diminished portal flow in the peripheral zone of the liver might have played a role in the pathogenesis of solitary necrotic nodules [31].

Previous authors have reported high signal intensity on T2-weighted images in two patients [14, 15] and arterial enhancement with cross-sectional imaging [5, 14, 18] and angiography [13, 20]. All of our cases showed low signal intensity on T2-weighted images and lack of enhancement. We postulate that these differences can be explained by different time points of observation in the evolution of solitary necrotic nodules. Early in their development, lesions show active inflammatory changes and angiogenesis that might be responsible for the high signal intensity on T2-weighted images [15] and the enhancement shown after contrast injection [13]. At a later stage, necrosis and devascularization can explain the different imaging appearances observed in our study [16].

We believe that we have shown the natural history of solitary necrotic nodules. In those patients whom we followed up for extended periods, we were able to show progressive diminution in size in all cases and metamorphosis into a calcified lesion in three cases. Two other patients in this study had calcified lesions. We speculate that these two cases likely would have appeared as noncalcified, nonenhancing lesions if imaged earlier. We believe that a prospective study evaluating the morphologic evolution of a larger number of solitary necrotic nodules at the initial stage (when calcifications have not developed yet) would be beneficial in confirming this hypothesis.

In two review articles [32, 33] listing the causes of calcified liver lesions, no mention was made of solitary necrotic nodules as a potential cause of hepatic calcifications. However, our results show that solitary necrotic nodules should be included as one of the potential causes of liver calcifications.

It is important to recognize the limitations of our study. The numbers reported are limited because they are relatively small, reflecting the rareness of this condition and

necessitating a retrospective study design. Another limitation is that cases collected from multiple institutions over many years lack uniformity with regard to imaging and pathologic analysis. A further limitation is that not every patient and every lesion underwent imaging with all three cross-sectional imaging techniques.

In conclusion, solitary necrotic nodules are usually small, solitary lesions mostly found under the liver capsule of the right lobe and showing hypoattenuation on CT and hypointensity on both T1- and T2-weighted MRI. Lack of enhancement after IV contrast injection should alert the radiologist to a possible diagnosis of solitary necrotic nodule and lead to pathologic confirmation. The evolution toward calcification is a further clue to this diagnosis.

References

1. Shepherd NA. Solitary necrotic nodule. *J Clin Pathol* 1990; 43:348–349
2. Berry CL. Solitary "necrotic nodule" of the liver: a probable pathogenesis. *J Clin Pathol* 1985; 38:1278–1280
3. Sundaresan M, Lyons B, Akosa AB. Solitary necrotic nodule of the liver: an aetiology reaffirmed. *Gut* 1991; 32:1378–1380
4. Tsui WM, Yuen RW, Chow LT, Tse CC. Solitary necrotic nodule of the liver: parasitic origin? *J Clin Pathol* 1992; 45:975–978
5. Alfieri S, Carriero C, Doglietto GB, Pacelli F, Crucitti F. Solitary necrotic nodule of the liver: diagnosis and treatment. *Hepatogastroenterology* 1997; 44:1210–1211
6. De Luca M, Luigi B, Formisano C, et al. Solitary necrotic nodule of the liver misinterpreted as malignant lesion: considerations on two cases. *J Surg Oncol* 2000; 74:219–222
7. Shepherd NA, Lee G. Solitary necrotic nodules of the liver simulating hepatic metastases. *J Clin Pathol* 1983; 36:1181–1183
8. Carella R, Fortunato C, Gubinelli M, D'Errico A, Mancini AM. Solitary necrotic nodule of the liver simulating a metastasis [in Italian]. *Pathologica* 1993; 85:573–577
9. Clouston AD, Walker NI, Prociv P. Parasitic origin of a solitary necrotic nodule of the liver. (abstr) *J Clin Pathol* 1993; 46:578
10. Desai S, Prabhu SR, Shrividya S. Fibrosing necrotic nodule of the liver. *Indian J Gastroenterol* 1995; 14:23–24
11. Nakanuma Y. Non-neoplastic nodular lesions in the liver. *Pathol Int* 1995; 45:703–714
12. De Franco A, Maresca G, De Gaetano AM, Giovannini I, Chiarla C, Marano P. Dynamic computed tomography in the characterization of focal hepatic lesions [in Italian]. *Radiol Med (Torino)* 1996; 91:91–100
13. Grazi GL, Mazziotti A, Gruttadauria S, Jovine E, Principe E, Cavallari A. Solitary necrotic nodules of the liver. *Am Surg* 1998; 64:764–767
14. Yoon KH, Yun KJ, Lee JM, Kim CG. Solitary necrotic nodules of the liver mimicking hepatic metastasis: report of two cases. *Korean J Radiol* 2000; 1:165–168
15. Iwase K, Higaki J, Yoon HE, et al. Solitary necrotic nodule of the liver. *J Hepatobiliary Pancreat Surg* 2002; 9:120–124
16. Colagrande S, Politi LS, Messerini L, Mascalchi M, Villari N. Solitary necrotic nodule of the liver: imaging and correlation with pathological features. *Abdom Imaging* 2003; 28:41–44
17. Koea J, Taylor G, Miller M, Rodgers M, McCall J. Solitary necrotic nodule of the liver: a riddle that is difficult to answer. *J Gastrointest Surg* 2003; 7:627–630
18. Marongiu L, Capra F, Cautero N, Pinna AD. Solitary necrotic nodule of the liver: diagnostic and therapeutic considerations regarding a case. *Chir Ital* 2004; 56:567–570
19. Glas L, Guyennon A, Chomel S, et al. What is your diagnosis? Solitary necrotic nodule of the liver [in French]. *J Radiol* 2006; 87:676–679
20. Imura S, Miyake K, Ikemoto T, et al. Rapid-growing solitary necrotic nodule of the liver. *J Med Invest* 2006; 53:325–329
21. Wang Y, Yu X, Tang J, et al. Solitary necrotic nodule of the liver: contrast-enhanced sonography. *J Clin Ultrasound* 2007; 35:177–181
22. Chen Z, Ni JL, Liu LY, Yan JJ, Huang L, Yan YQ. Diagnosis and treatment for solitary necrotic nodule of the liver: report of 15 patients [in Chinese]. *Zhonghua Wai Ke Za Zhi* 2007; 45:1328–1330
23. Couinaud C. *Le foie: études anatomiques et chirurgicales.* Paris, France: Masson, 1957
24. Cotran RS, Kumar V, Robbins SL. Cell injury and cellular death. In: Cotran RS, Kumar V, Robbins SL, eds. *Robbins pathologic basis of disease*, 5th ed. Philadelphia, PA: W. B. Saunders, 1994: 379–430
25. Yeldandi AV, Kaufman DG, Reddy JD. Cell injury and cellular adaptations. In: Damjanov I, Linder J, Anderson WAD, eds. *Anderson's pathology.* New York, NY: Mosby, 1996:374–375
26. Bartolozzi C, Lencioni R, Caramella D, Mazzeo S, Ciancia EM. Treatment of hepatocellular carcinoma with percutaneous ethanol injection: evaluation with contrast-enhanced MR imaging. *AJR* 1994; 162:827–831
27. Outwater E, Tomaszewski JE, Daly JM, Kressel HY. Hepatic colorectal metastases: correlation of MR imaging and pathologic appearance. *Radiology* 1991; 180:327–332
28. Maetani Y, Itoh K, Watanabe C, et al. MR imaging of intrahepatic cholangiocarcinoma with pathologic correlation. *AJR* 2001; 176:1499–1507
29. Murphy-Lavallee J, Jang HJ, Kim TK, Burns PN, Wilson SR. Are metastases really hypovascular in the arterial phase? The perspective based on contrast-enhanced ultrasonography. *J Ultrasound Med* 2007; 26:1545–1556
30. Namasivayam S, Martin DR, Saini S. Imaging of liver metastases: MRI. *Cancer Imaging* 2007; 7:2–9
31. Itai Y, Matsui O. Blood flow and liver imaging. *Radiology* 1997; 202:306–314
32. Paley MR, Ros PR. Hepatic calcification. *Radiol Clin North Am* 1998; 36:391–398
33. Stoupis C, Taylor HM, Paley MR, et al. The rocky liver: radiologic–pathologic correlation of calcified hepatic masses. *RadioGraphics* 1998; 18:675–685